



Rice husk ash – A valuable reinforcement for high density polyethylene

E.P. Ayswarya, K.F. Vidya Francis, V.S. Renju, Eby Thomas Thachil*

Department of Polymer Science and Rubber Technology, Cochin University of Science and Technology, Kochi, 682 022 Kerala, India

ARTICLE INFO

Article history:

Received 15 January 2012

Accepted 19 April 2012

Available online 27 April 2012

Keywords:

A. Composites

Thermoplastic

E. Mechanical

G. Scanning electron microscopy

ABSTRACT

This paper presents the results of a study on the use of rice husk ash (RHA) for property modification of high density polyethylene (HDPE). Rice husk is a waste product of the rice processing industry. It is used widely as a fuel which results in large quantities of RHA. Here, the characterization of RHA has been done with the help of X-ray diffraction (XRD), Inductively Coupled Plasma Atomic Emission Spectroscopy (ICPAES), light scattering based particle size analysis, Fourier transform infrared spectroscopy (FTIR) and Scanning Electron Microscope (SEM). Most reports suggest that RHA when blended directly with polymers without polar groups does not improve the properties of the polymer substantially. In this study RHA is blended with HDPE in the presence of a compatibilizer. The compatibilized HDPE-RHA blend has a tensile strength about 18% higher than that of virgin HDPE. The elongation-at-break is also higher for the compatibilized blend. TGA studies reveal that uncompatibilized as well as compatibilized HDPE-RHA composites have excellent thermal stability. The results prove that RHA is a valuable reinforcing material for HDPE and the environmental pollution arising from RHA can be eliminated in a profitable way by this technique.

© 2012 Elsevier Ltd. All rights reserved.

1. Introduction

High density polyethylene (HDPE) is one of the most important commercial polyolefins. It finds widespread use in such applications as household appliances, automobiles, aeronautics and packaging. HDPE has excellent low temperature toughness, chemical resistance, good dielectric properties and relatively high softening temperature. But it has poor weatherability [1]. In order to reduce cost or enhance physical and mechanical properties additives or fillers can be added to HDPE. These fillers may be natural byproducts (natural fibers, sawdust, rice husk ash, etc.) or commercial fillers such as carbon black, precipitated silica and talc [2,3].

According to FAO statistical data, the world rice production was approximately 697.9 million tones in 2010 [4]. Raw rice husk contain 35% cellulose, 25% hemicellulose, 20% lignin, 17% ash (94% silica) and about 3% by weight of moisture [5]. Most of the rice husk is used for such mundane applications as bedding material for animals, fuel and landfill. The novel use of rice husk and RHA as fillers in thermoplastic polymer composites has attracted much attention recently [6–8]. Depending upon the incineration conditions, two types of ash are produced i.e., white rice husk ash (WRHA) and black rice husk ash (BRHA) [9]. White RHA has smaller specific surface area (1.4 m²/g) than the black colored one and its particle size is reported to be about 50 μm [6]. In the following sections, RHA refers to specifically white RHA.

RHA is thermally stable and a tough material possessing high specific properties. It has approximately 55–97% silica content distributed between crystalline and amorphous forms. Combustion conditions determine the extent of crystallinity. Its application as a filler in thermoplastics mainly depends on purity and particulate characteristics. Environmental pollution and the necessity to conserve energy and material resources have encouraged the use of RHA in applications such as fillers in cement and fertilizers, catalyst carriers and in the production of pure silica, silica gels, geopolymer and filled polymers [10,11].

The use of RHA as a filler in HDPE has the twofold advantage of reducing the pollution potential of RHA and modifying the properties of HDPE by a cost effective and reliable method. This work has been undertaken with this objective in mind.

Silica is the predominant component of RHA with trace amounts of various elements such as potassium, sodium, magnesium and calcium also present [12]. The fine particle size (<50 μm), irregular shape and porosity facilitate the use of silica ash as a filler in polymers. The presence of hydroxyl groups on the ash particles is advantageous in the case of polymers containing polar groups. Physical properties such as topography, shape and size are known to affect the filler reinforcing character in any resin [13]. The particle morphology and particle size are well correlated with aggregation tendencies and could also be linked to dispersive nature. The major impurity is a form of trapped carbon. The impurity reduces the filler efficiency in composites [14].

Addition of RHA to a thermoplastic increases the stiffness but tends to reduce strength and toughness [15]. Most silicate fillers

* Corresponding author. Tel.: +91 484 2575723; fax: +91 484 2577747.

E-mail address: ethachil@cusat.ac.in (E.T. Thachil).

have on their surface hydrophilic hydroxyl (-OH groups) or silanol groups and readily adsorb moisture from the environment [5]. These hydroxyl groups increase the filler aggregation and consequently, greater energy is required to break them into smaller agglomerates. For better matrix–filler interactions, filler particles must be wet by the resin. Most polymer melts, being hydrophobic and highly viscous, do not wet the filler surface effectively. This leads to incompatibility and a poorly formed interface between the polymer and filler [16,17]. Coupling or compatibilizing agents have been used to improve dispersion, adhesion and compatibility between the hydrophobic and hydrophilic systems. These agents modify the interface by interacting with both the filler and the polymer, thus forming a link between these components [18]. RHA has also the ability to increase the thermal stability of the composites.

The specific objectives of this experimental study were to prepare HDPE-RHA composites, test the properties and explore ways to get optimal performance from the composites. An attempt has been made to improve the compatibility between RHA and HDPE by subjecting the polymer to a chemical modification.

2. Experimental details

2.1. Materials

High density polyethylene was supplied by Reliance Industries Limited, Mumbai, India. It has a melt flow index (MFI) of 9.65 g/10 min (190 °C/2.16 kg). Maleic anhydride (MA) and dicumyl peroxide (DCP) were supplied by SD fine-chem. Limited, Mumbai.

2.2. Preparation of rice husk ash

Rice husk was collected from rice mills. It was washed clean with distilled water to remove grit and dried in an oven at a temperature of 100 °C for 2 h. It was subsequently burnt in five batches in a muffle furnace for 6 h each at five different temperatures (500 °C, 550 °C, 600 °C, 650 °C and 700 °C). This incineration time was found to give concordant values of ash content at each temperature.

2.3. Compatibilization

The compatibilizer (MA-g-HDPE) was the product of a grafting reaction between maleic anhydride (MA) and HDPE with the help of dicumyl peroxide (DCP) initiator at 145 °C. The reaction was conducted by melt mixing the above ingredients in a Thermo Haake PolyLab system equipped with roller rotors. The MA-g-HDPE obtained was then used as an ingredient in the preparation of HDPE-RHA blends in order to improve compatibility between HDPE and RHA.

2.4. Preparation of HDPE-RHA composites

A few initial studies were done on HDPE/RHA samples without compatibilizer. For this only the ash prepared at 550 °C was used as this temperature gave a mostly amorphous ash. Amorphous ash is reported to possess greater reinforcing properties because of higher reactivity [19]. For preparing compatibilized blends, HDPE was mixed with the compatibilizer (MA-g-HDPE) and RHA in a Thermo Haake PolyLab system earlier mentioned under the same conditions employed for preparing the compatibilizer. RHA was initially heated for 1 h at 120 °C in an air oven to drive away any absorbed moisture. Different amounts of the dry RHA (0, 0.5, 1, 1.5, 2 and 2.5 wt.%) and a constant amount of compatibilizer (constituting 15% of the weight of the total blend) were blended to HDPE and the resulting composites were tested to find the optimum percentage of RHA.

2.5. Preparation of test specimens

The test specimens were prepared from the blends by moulding in an electrically heated hydraulic press for 5 min at 150 °C under a pressure of 20 Mpa. After moulding, the samples were cooled down to room temperature under pressure. Rectangular shaped specimens were cut from the moulded sheets and used for testing.

2.6. Mechanical testing

Mechanical properties were evaluated using a Shimadzu Auto-graph AG-I Series Universal Testing Machine at a crosshead speed of 50 mm/min according to ASTM D 882 (2002) [20]. Six specimens were used and the average was calculated in each case. These tests provided the ultimate tensile strength, elongation-at-break and Young's modulus values of the composites.

2.7. Measurement of melt flow index (MFI)

The MFI of uncompatibilized HDPE-RHA and compatibilized HDPE-RHA composites were determined using a CEAST Modular Line Melt Flow Indexer, according to ASTM D1238 (190 °C/2.160 kg) [21].

2.8. Chemical analysis of RHA

Elemental and chemical compositions of RHA were obtained using Inductively Coupled Plasma Atomic Emission Spectroscopy (ICPAES). Samples for ICPAES were prepared by first drying the ash in an oven (120 °C, 1 h) and then dissolving approximately 100 mg of dried ash in 4 ml of reagent grade, concentrated hydrochloric acid. The mixture was left standing for a couple of hours for complete dissolution. This solution was later diluted to approximately 100 g using distilled water so that the concentration of various elements was within the linear range of detection for the ICPAE Spectrometer. The solution was analyzed for concentrations of P, K, Ca, Mg, S, Zn, Mn, B, Al, Fe, Si, and Na by a Thermo Electron IRIS INTREPID II X SP DUO spectrometer.

2.9. Particle size analysis

2.9.1. X-ray diffraction (XRD)

Finely ground RHA mounted on a glass slide was used for X-ray diffraction studies. The samples were analyzed in a Bruker AXS D8 Advance X-ray Powder Diffractometer.

2.9.2. Light scattering

The average particle size of RHA was determined using a particle size analyzer. The sample for particle size analysis was prepared by dispersing 500 mg of RHA in a 5% solution of potassium oleate and sonicating for 6 h. From this, about 3 ml of solution was used for testing. The solution was analyzed by Malvern Zetasizer (Model Nano-S), manufactured by Malvern Instruments, UK.

2.10. Fourier transform infrared spectroscopy (FTIR)

FTIR spectra of representative samples were recorded on a Thermo Nicolet FTIR Spectrometer Model Avatar 370. Samples in the form of thin films, <1 mm thickness, were employed.

2.11. Thermo gravimetric analysis (TGA)

Thermo gravimetric analysis of the samples was carried out in a TGA Q-50 thermal analyzer (TA Instruments) under nitrogen atmosphere. Nitrogen was employed in order to remove all corrosive

gases evolved from the degraded materials and to avoid thermo oxidative degradation. The samples were heated from room temperature to 700 °C at a heating rate of 20 °C/min and a nitrogen gas flow rate of 40–50 cm³/min. Sample weights varied from 10 to 15 mg. The onset of degradation temperature, the temperature at which weight loss is maximum (T_{max}) and residual weight in percentage, etc. were noted.

2.12. Morphology

The morphological characterization of RHA and tensile fractured surfaces of the composite specimens were carried out using a JEOL Model JSM 6390LV Scanning Electron Microscope (SEM). The samples were subjected to gold sputtering prior to electron microscopy to give the necessary conductivity.

3. Results and discussions

3.1. RHA characterization

Fig. 1 shows the XRD pattern of RHA prepared at different temperatures. The sharp peaks in the figure represent crystalline components while the broad peaks indicate amorphous fractions. The peaks are mostly sharp at higher temperatures (>650 °C). It has been pointed out that RHA turns more crystalline at higher temperatures [13]. Using Scherrer's equation [22], the average particle size of RHA was found to be 263–270 nm.

ICPAES (Table 1) indicates that RHA mainly consists of silicon, calcium, magnesium and potassium. Small amounts of aluminum and iron are also present. Light scattering studies (Table 2) reveal that about 9.6% particles are below 100 nm, 60% in the range 100–200 nm, 25.6% in the range 200–300 nm and 5.6% above 300 nm (up to 531 nm).

3.2. Mechanical properties of HDPE-RHA composites

Fig. 2 shows the effect of RHA content on the tensile strength, elongation at break and Young's modulus of uncompatibilized HDPE/RHA composites during initial studies. Tensile strength de-

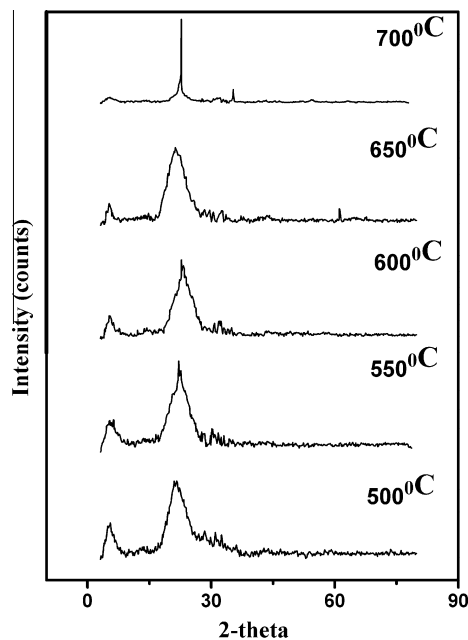


Fig. 1. XRD of different temperatures RHA.

Table 1

Composition of RHA (ICPAES) prepared at 550 °C.

Component	Weight (%)
Silicon	64.81
Aluminum	0.26
Boron	2.09
Calcium	4.05
Iron	0.95
Potassium	20.56
Magnesium	5.58
Manganese	0.28
Sodium	1.36
Zinc	0.06

Table 2

Particle size of RHA (550 °C) by light scattering.

RHA particle size (nm)	Mean volume (%)
58.77	0.2
68.06	0.6
78.82	2.7
91.28	6.1
105.7	9.2
122.4	11.6
141.8	13.4
164.2	13.5
190.1	12.4
220.2	10.7
255	8.7
295.3	6.2
342	3.4
396.1	1.2
458.7	0.2
531.2	0.8

creases steadily with increasing filler loading due to the incompatibility of the matrix with the filler system. The absence of a coupling agent results in poor adhesion of the ash particulates to the matrix. Weak interfacial regions imply that the filler particles cannot carry any of the load applied to the composites and the entire stress has to be carried solely by the matrix material. Because of poor wetting, the filler particles and agglomerates retain air in their hollow spaces, introducing porosity to the internal structure of the composites. Agglomeration of the filler particles and dewetting of the polymer at the interphase aggravate the situation by creating stress concentration points. This leads to reduced tensile

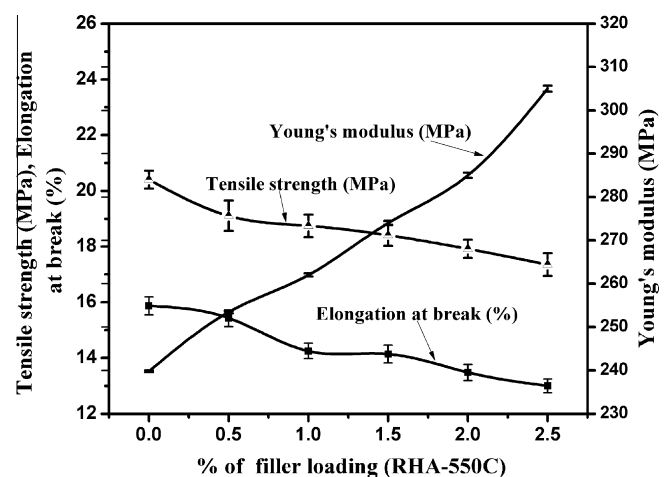


Fig. 2. Tensile strength, Elongation at break and Young's modulus vs % filler loading in uncompatibilized HDPE.

strength [23,24]. Elongation at break predictably decreases with increasing filler loading because cracks travel through the weaker interfacial regions and the composite fractures at lower values of elongation [25]. The Young's modulus increases steadily with increasing filler loading. According to Neilsen, the addition of rigid and stiff particulate fillers would increase the modulus of the composites because of increasing restrictions on the mobility of the polymer molecules [26]. Such behavior from incompatible filler materials is wellknown [27–29].

Scheme 1 shows the mechanism by which a free radical is generated on the HDPE chain by DCP and subsequent reaction with MA to give a functionalized HDPE molecule. This polymer chain then reacts with silanol groups on the ash surface opening the anhydride ring and facilitating extensive hydrogen bonding between HDPE chains.

Fig. 3 shows the effect of changing incineration temperature of RHA on the tensile strength, elongation at break and Young's modulus of the compatibilized HDPE/RHA blend. From the figure, ash at 550 °C gives the highest tensile strength and elongation at break for composites. Moreover, the reactivity of RHA is known to be higher at lower temperatures [19]. So further studies were done using only the ash prepared at 550 °C. Young's modulus of the composites increases with increasing filler loading. This is a common observation with filled materials [30]. In one of our previous studies it was found that at 15% compatibilizer (MA-g-HDPE) the mechanical properties of virgin HDPE (without filler) were maximum [31]. Hence the same compatibilizer % was retained for all studies.

Fig. 4 shows the effect of RHA content on the tensile strength, elongation at break and Young's modulus of compatibilized HDPE/RHA composites. The behavior of the composite in the presence of the compatibilizer is vastly superior. At 1.5% ash the improvement in tensile strength is as much as 22% as against a reduction of 13% in the absence of the compatibilizer. The use of the compatibilizer has proven to be effective in enhancing the dispersion, adhesion and compatibility of the filler with the hydrophobic matrix. The tensile strength of the compatibilized HDPE-ash composite also shows an increasing tendency with increasing filler loading until 1.5%. The breaking elongation of the composite also reaches a maximum at 1.5 wt.% of ash. When the composites are

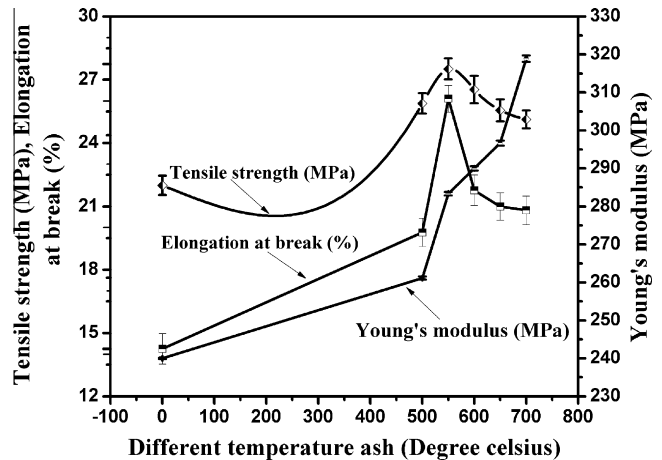


Fig. 3. Tensile strength, Elongation at break and Young's modulus vs % of different temperatures ash in compatibilized HDPE.

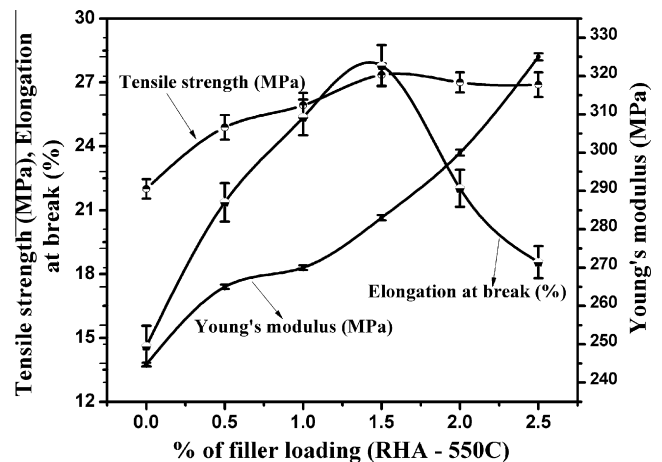
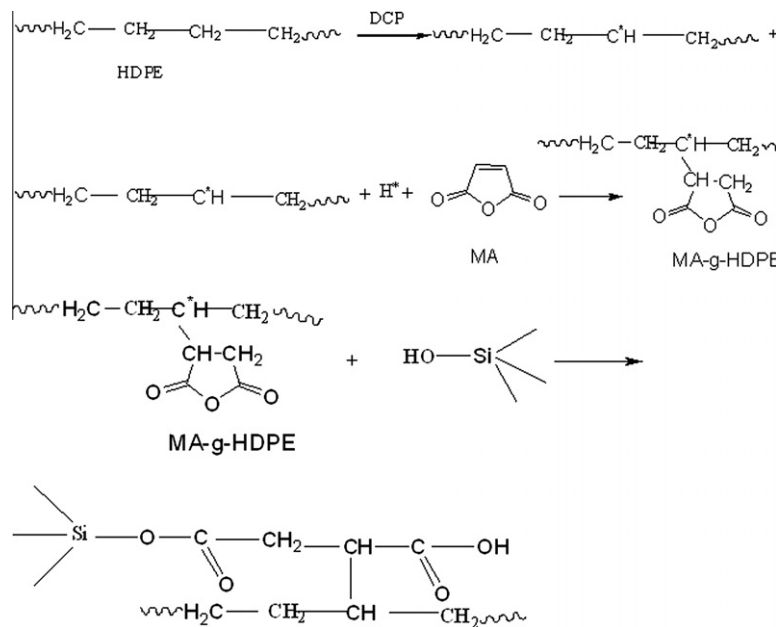


Fig. 4. Tensile strength, Elongation at break and Young's modulus vs % filler loading in compatibilized HDPE.



Scheme 1. Reaction between MA-g-HDPE and silanol group in RHA.

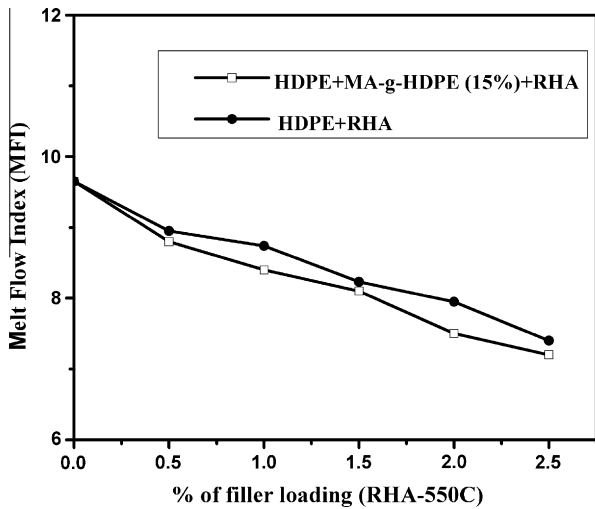


Fig. 5. Melt flow index vs % filler loading in HDPE.

under exterior stress, the filler helps to distribute the stress evenly and delay the rupture of the material. Young's modulus of the composites increases with increasing filler loading. The interfacial adhesion is increased by the presence of the compatibilizer and the high surface area of the filler gives rise to increased modulus and strength.

3.3. Melt flow measurement

Fig. 5 shows the variation of the melt flow index of HDPE/RHA blends in the presence as well as absence of compatibilizer. Low melt flow index indicates a higher melt viscosity [32]. Addition of compatibilizer was expected to increase the viscous as well as elastic response of the system by improving filler-matrix interaction. The result is in agreement with the recognized ability of maleated polyethylene to strengthen the intermolecular forces between the polymer chains via chemical and physical bonds and also to restrict chain mobility by the presence of the anhydride ring [33]. The ability of anhydride rings to interact with silanol groups has already been mentioned.

3.4. FTIR

Fig. 6 shows the spectra of RHA and compatibilized HDPE-RHA composites. The FTIR spectrum shows a peak at 1106.16 cm^{-1}

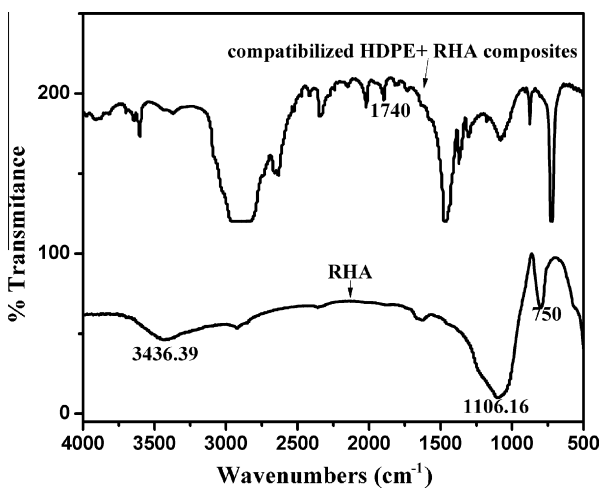


Fig. 6. FTIR of RHA and compatibilized composites.

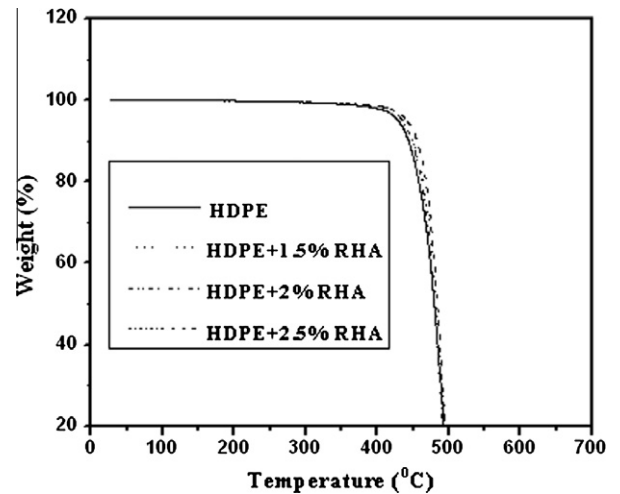


Fig. 7. Thermogram of HDPE-RHA uncompatibilized composites.

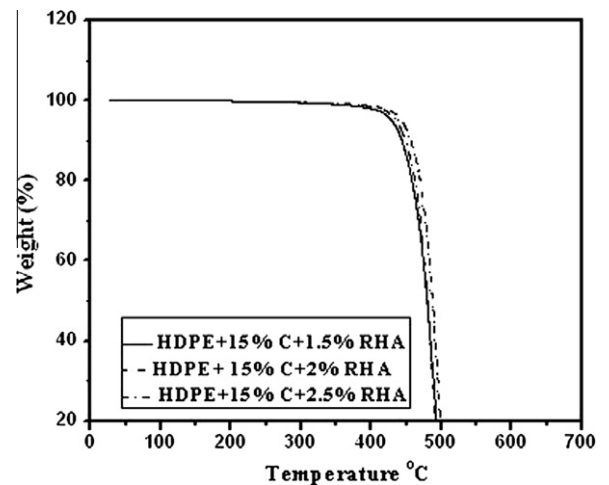


Fig. 8. Thermogram of compatibilized HDPE-RHA composites.

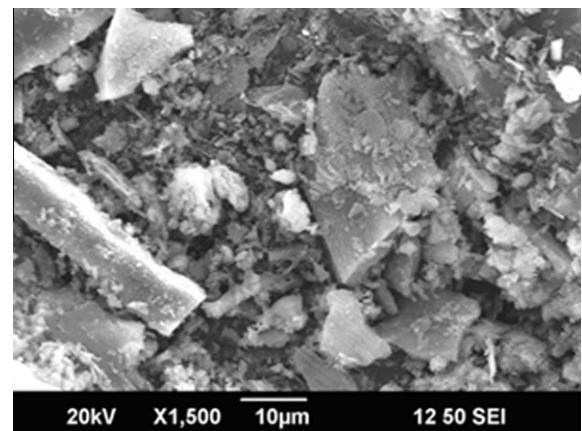


Fig. 9. SEM image of RHA.

corresponding to Si—O—Si stretching vibration [34]. The peak at 750 cm^{-1} shows vibration of Al_2O_3 [35]. The peak at 3436.39 cm^{-1} indicates the presence of O—H group in the RHA [34] arising from silanol molecules. The spectrum of the compatibilized composite shows a peak at 1740 cm^{-1} assignable to symmetric stretching of

Table 3
TGA analysis of HDPE and HDPE-RHA composites.

Sample	Onset T (°C)	Peak T (°C)	End T (°C)	10% weight loss (°C)	20% Weight loss (°C)	50% weight loss (°C)	Residue (%)
HDPE	384.39	482.73	502.02	441.11	455.18	474.55	0.33
HDPE + 0.5% RHA	412.55	491.82	513.97	450.29	472.23	486.49	0.82
HDPE + 1% RHA	414.98	492.91	511.33	453.97	473.69	487.52	1.32
HDPE + 1.5% RHA	413.57	493.54	511.51	455.07	473.37	486.39	1.802
HDPE + 2% RHA	415.38	495.14	513.30	457.81	472.04	490.50	2.30
HDPE + 2.5% RHA	422.76	497.54	517.35	458.88	475.49	491.57	2.882
HDPE + 15%C + 1.5% RHA	420	497.31	514.68	458.05	472.40	490.42	1.780
HDPE + 15%C + 2% RHA	421.56	500.74	518.42	462.88	477.13	494.31	2.301
HDPE + 15%C + 2.5% RHA	430.96	501.64	518.56	467.82	480.36	496.42	2.812

C=O group present in ester moieties. The C=O group present in the anhydride ring will show absorbance at a different wave number 1830 cm^{-1} [36] which is not noticeable in the spectrum. This indicates that the functional groups of MA-g-HDPE react with the hydroxyl groups of RHA (Scheme 1) leading to covalent bonding and esterification reactions [37].

3.5. Thermo gravimetry

Figs. 7 and 8 show the thermograms of pure HDPE, three cases of RHA/HDPE in the absence of compatibilizer and three cases of RHA/HDPE in the presence of 15% compatibilizer. The thermal degradation of HDPE can take place through random chain scission and a radical chain mechanism [38,39]. The established mechanism for polyethylene involves formation of free radicals and abstraction of hydrogen from the polymer chains leading to a molecular weight decrease and finally to the formation of volatile products. Polyethylene decomposes into a large number of paraffinic and olefinic compounds without residue [40].

The thermograms (Fig. 7, without compatibilizer) show only moderate variation. But the maximum temperature of degradation is seen to increase with RHA content. The variation somewhat increases in the presence of the compatibilizer (Fig. 8) showing that there is a marginal improvement in thermal stability on addition of compatibilizer.

Table 3 shows concisely information obtained from the thermograms. The thermal degradation of virgin HDPE starts at $384.39\text{ }^{\circ}\text{C}$ and 100% degradation are observed at $502.02\text{ }^{\circ}\text{C}$. HDPE shows maximum degradation at $482.73\text{ }^{\circ}\text{C}$. Addition of rice husk ash into HDPE increases this to $491.82\text{--}497.54\text{ }^{\circ}\text{C}$. Enhancement of thermal stability of the rice husk ash composites is attributed to the organic/inorganic interaction between the polymer and rice husk ash where inorganic filler delays the volatilizations of the products generated at the temperature of carbon–carbon bond scission of the polymer matrix [41]. The presence of the filler restricts the mobility of the polymer chains and thereby delays the thermal degradation [42]. The inorganic ash can also absorb the heat generated during the degradation and help to decelerate the overall degradation process.

The compatibilized blends show marginally superior thermal stability by virtue of reduced segmental motion of the polymer chains. The compatibilizer has the effect of making the chains less mobile due to interactions between the HDPE and RHA. This has the effect of making the blend less susceptible to thermal degradation. The reduced MFI of compatibilized blends is also suggestive of this.

3.6. Scanning electron microscopy (SEM)

Fig. 9 shows that RHA particles are of irregular shape and have a tendency to form agglomerates [5]. A micrograph of the failure surface of RHA filled-HDPE without MA-g-HDPE is shown in Fig. 10a.

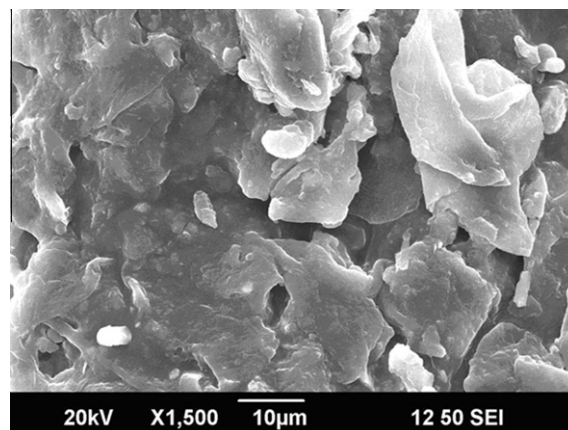


Fig. 10a. SEM image of HDPE-RHA composite.

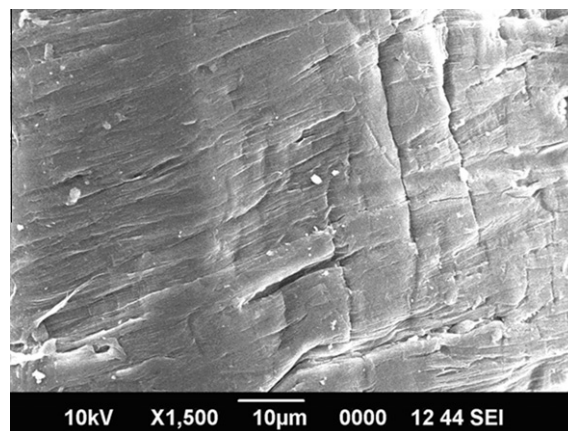


Fig. 10b. SEM image of compatibilized HDPE-RHA composite.

RHA particles in the composite are found to be of widely different sizes presumably due to agglomeration and nonhomogeneous dispersion. Inadequate wetting can also be responsible for this. In the absence of wetting the particles tend to stick together rather than getting distributed evenly in the melt. Fig. 10b is a micrograph of the surface of the RHA filled-HDPE composites compatibilized by MA-g-HDPE. The presence of MA-g-HDPE leads to a homogenous dispersion of RHA and improved wettability. The wavy pattern is an indication of greater energy absorption.

4. Conclusion

The results prove that RHA, a pollutant, can be used as reinforcing filler in the processing of HDPE. It can be incorporated into

HDPE by the melt blending process. In the absence of a compatibilizer, blends of HDPE and rice husk ash show mechanical properties inferior to the base polymer. But a compatibilizer consisting of MA-g-HDPE greatly improves the mechanical properties, viz. tensile strength, modulus and elongation of RHA-HDPE composites. The compatibilized blend is also found to have a more homogeneous structure. The best mechanical properties are observed at 1.5% RHA and 15% compatibilizer. The technique provides a method for gainful utilization of RHA and a cheap and profitable way to strengthen HDPE.

Acknowledgment

The authors wish to thank Dr. Siby Varghese for helping with particle size analysis at RRII, Kottayam, Kerala.

References

- [1] Zebarjad SM, Sajjadi SA, Tahani M, Lazzeri A. A study on thermal behaviour HDPE/CaCO₃ nanocomposites. *J AMME* 2006;17:173–6.
- [2] Saheb DN, Jog JP. Natural fibre polymer composites: a review. *Polym Adv Technol* 1999;18:351–63.
- [3] Aigbodoin VS, Hassan SB, Agunsove JO. Effect of bagasse ash reinforcement on dry sliding wear behaviour of polymer matrix composites. *JMAD* 2012;33:322–32.
- [4] Rice market monitor. Trade and markets division, food and agriculture organization of the united nations. *Rice market monitor*; 2010; 13: 1–37.
- [5] Chaudhary DS, Jollands MC, Cser F. Understanding rice hull ash as fillers in polymers: a review. *Silicon Chem* 2002;1:281–9.
- [6] Ahmad Fuad MY, Ismail Z, Mansor MS, Mohd Ishak ZA, Mohd Omar AK. Mechanical properties of rice husk ash/polypropylene composites. *Polym J* 1995;27:1002–15.
- [7] Siriwardena S, Ismail H, Ishiaku US. A Comparison of the mechanical properties and water absorption behavior of white rice husk ash and silica filled polypropylene composites. *J Reinf Plast Compos* 2003;22:1645–66.
- [8] Turmanova S, Dimitrova A, Vlaev L. Comparison of water absorption and mechanical behaviors of polypropylene composites filled with rice husk ash. *Polym-Plast Technol Eng* 2008;47:809–18.
- [9] Zhao Qiang, Zhang Baoqing, Hui Quana, Richard Yam CM, Richard Yuen KK, Robert Li KY. Flame retardancy of rice husk-filled high-density polyethylene ecocomposites. *Compos Sci Technol* 2009;69:2675–81.
- [10] Kord Behzad. Nano filler reinforcement effects on the thermal, dynamic mechanical and morphological behaviour of HDPE/rice husk flour composites. *Bioresources* 2011;6:1351–8.
- [11] Vlaev Lyubomir, Turmanova Sevdalina, Dimitrova Antonia. Kinetics and thermodynamics of water adsorption onto rice husks ash filled polypropylene composites during soaking. *J Polym Res* 2009;16:151–64.
- [12] Kalapathy U, Proctor A, Shultz J. Production and properties of flexible sodium silicate films from rice hull ash silica. *Bioresour Technol* 2000;72:99–106.
- [13] Omatola KM, Onojah AD. Elemental analysis of rice husk ash using X-ray fluorescence technique. *Int J Phys Sci* 2009;4:189–93.
- [14] Krishnarao RV, Subrahmanyam J, Jagadish Kumar T. Studies on the formation of black particles in rice husk silica ash. *J Eur Ceram Soc* 2001;12:99–104.
- [15] Fuad MA, Jamaludin M, Ishak ZAM, Omar AKM. Rice husk ash as a fillers in polypropylene: a preliminary study. *Intan J Polym Mater* 1993;19:75–92.
- [16] Nunes RCR, Fonseca JLC, Pereira MR. Polymer-filler interactions and mechanical properties of a polyurethane elastomer. *Polym Test* 2000;19:93–103.
- [17] Kahlf KF, Ward AA. Use of rice husk ash as potential filler styrene butadiene rubber/linear low density polyethylene blends in presence of maleic anhydride. *JAMD* 2010;31:2414–21.
- [18] Panthapulakkal S, Law S, Sain M. Enhancement of processability of rice husk filled high-density polyethylene composite profiles. *J Thermoplast Compos Mater* 2005;18:445–58.
- [19] Chandrasekhar S, Satyanarayana KG, Pramada PN, Raghavan P. Review processing, properties and applications of reactive silica from rice husk- an overview. *J Mater Sci* 2003;38:3159–68.
- [20] ASTM D882-10, D882-10 Standard test method for tensile properties of thin plastic sheeting, volume 08.01, ICS number code 83.140.10 (films and sheets).
- [21] ASTM D1238-10, D1238-10 Standard test method for melt flow rates of thermoplastics by extrusion plastometer, volume 08.01, ICS number code 83.080.20 (thermoplastic material).
- [22] Thomas Paul K, Satpathy SK, Manna I, Chakraborty KK, Nando GB. Preparation and characterization of nano structured materials from fly ash: a waste from thermal power stations, by high energy ball milling. *Nanoscale Res Lett* 2007;2:397–404.
- [23] Nielsen LE, Robert RF. Mechanical properties of polymers and composites. 2nd ed. New York: Marcel Dekker; 1974.
- [24] Manson JA, Sperling LH. Polymer blends and composites. 15th ed. New York: Plenum; 1976.
- [25] Ahamed Fuad MY, Shukor R, Mohd Ishak ZA, Mohad omar AK. Rice husk ash as a filler in polypropylene: effect of wax and silane coupling agents. *Plast Rubber Compos Appl* 1994;21:225–35.
- [26] Ismail H, Megha L, Abdul Khalil HPS. Effect of a silane coupling agent on the properties of white rice husk ash – polypropylene/natural rubber composites. *Polym Int* 2001;50:606–11.
- [27] Ismail H, Mohamad Z, Baker AA. A comparative study on processing, mechanical properties, thermo-oxidative aging, water absorption, and morphology of rice husk powder and silica fillers in polystyrene/styrene butadiene rubber blends. *Polym Plast Technol Eng* 2003;42:81–103.
- [28] Surayashastry Bose, Mahanwar PA. Effect of flyash on the mechanical, thermal, dielectric, rheological and morphological properties of filled nylon 6. *JMMCE* 2004;3:65–89.
- [29] Jayasree TK, Predeep P. Effect of fillers on mechanical properties of dynamically crosslinked styrene butadiene rubber/high density polyethylene blends. *J Elastom Plast* 2008;40:127–46.
- [30] Marcovich NE, Marcelo Villar A. Thermal and mechanical characterization of linear low density Polyethylene/wood flour composites. *J Appl Poly Sci* 2003;90:2775–84.
- [31] Ayswarya EP, Beena Abraham T, Thachil Eby Thomas. HDPE-ash nanocomposites. *J Appl Poly Sci* 2012;124:1659–67.
- [32] Stabik J, Suchon L, Rojek M, Szczepanik M. Investigation of processing properties of polyamide filled with hard coal. *JAMME* 2009;33:142–9.
- [33] Moayad Khalaf N, Ali Al-Mowali H, Georgius Adam A. Rheological studies of modified maleated polyethylene/medium density polyethylene blends. *MPJ* 2008;2:54–64.
- [34] Thongsang S, Sombatsompop N. Effect of NaOH and Si69 treatments on the properties of fly ash/natural rubber composites. *Polym compos* 2006;27:34–40.
- [35] Najib NN, Ismail H, Azura AR. Thermoplastic elastomer composites of palm ash-filled ethylene vinyl acetate/natural rubber blends: effects of palm ash loading and size. *Polym Plast Technol Eng* 2009;48:1062–9.
- [36] Sheshkali HRZ, Assempour H, Nazockdast H. Parameters affecting the grafting reaction and side reactions involved in the free radical melt grafting of maleic anhydride onto high-density polyethylene. *J Appl Poly Sci* 2007;105:1869–81.
- [37] Kim Hee-Soo, Lee Byoung-Ho, Choi Seung-Woo, Kim Sumin, Kim Hyun-Joong. Composites Part A 2007;38:1478–85.
- [38] Kim HS, Yang HS, Kim HJ, Park HJ. Thermogravimetric analysis of rice husk flour filled thermoplastic polymer composites. *J Therm Anal Calorim* 2004;76:395–404.
- [39] Paradise Melissa, Goswami Tarun. Carbon nanotubes – production and industrial applications. *JMAD* 2007;28:1477–89.
- [40] Chrissafis K, Paraskevopoulos KM, Pavlidou E, Bikiaris D. Thermal degradation mechanism of HDPE nanocomposites containing fumed silica nanoparticles. *Thermochim Acta* 2009;485:65–71.
- [41] Biswal Manoranjan, Mohanty Smita, Sanjaya Nayak K. Mechanical, thermal and dynamic-mechanical behaviour of banana fiber reinforced polypropylene nanocomposites. *Polym Compos* 2011;32:1190–201.
- [42] Ren Fang, Ren Peng-Gang, Di Ying-Ying, Chen De-Ming, Liu Gui-Guo. Thermal, mechanical and electrical properties of linear low-density polyethylene composites filled with different dimensional SiC particles. *Polym-Plast Technol Eng* 2011;50:791–6.